Computer modeling of $Ba_2RE^{3+}NbO_6$ (RE^{3+} = rare-earth and Y) compounds

Computer modeling of $Ba_2RE^{3+}NbO_6$ $(RE^{3+} = $ rare-earth and Y) compounds

C W A Paschoal[1] and E M Diniz[2]

[1] Departamento de Física, CCET, Universidade Federal do Maranhão, 65085-580, São Luís, MA, Brazil
[2] Departamento de Física, ICEx, Universidade Federal de Minas Gerais, PO Box 702, 30161-970, Belo Horizonte, MG, Brazil

E-mail: paschoal@ufma.br

Abstract
In this work we have performed atomistic simulations in $Ba_2RE^{3+}NbO_6$ (RE^{3+} = La, Ce, Nd, Pr, Pm, Sm, Eu, Gd, Tb, Dy, Y, Ho, Er, Tm, Yb and Lu) compounds in order to predict their physical properties and behavior under lanthanide substitutions. The potential model adopted describes very well the structural and dielectric properties of these materials. The dependence of the tolerance factor on their physical properties was investigated and the results indicate that the lattice energy, sound velocities and bulk modulus do not show morphotropic phase boundaries between the three phases in which these compounds crystallize. These observables have a linear dependence on the tolerance factor. Only the elastic constant shows morphotropic phase boundaries.

(Some figures in this article are in colour only in the electronic version)

1. Introduction

The perovskite structure is doubtless the most versatile ceramic host that has been investigated in material science. Since the crystal chemistry investigations of Goldschmidt [1], several substitutions have been performed in ABX_3 basic stoichiometry with the aim of obtaining new compounds with new physical properties. Thus, compounds with perovskite or related structure were obtained as metallic conductors, superconductors, ferroelectrics, relaxors, high dielectric constant materials, piezoelectrics and electrooptics amongst others, as was very well reviewed by Bhalla *et al* [2]. Also, there is an increasing interest in ionic conductors with perovskite structure being used as separator materials in solid oxide fuel cells [3]. Commonly, the complex perovskite structure is that obtained by multiple ion substitution at the A, B or X sites. These substitutions can imply order or disorder, depending on the statistical distribution of ions among the sites. There are two large complex perovskite families when the substitution occurs at the B site: $A(B'_{1/3}B''_{2/3})X_3$ or $A(B'_{1/2}B''_{1/2})X_3$. Both families have great applicability in integrated industrial devices. In particular, the $Ba(RE_{1/2}Nb_{1/2})O_3$ family, where RE is a

lanthanide ion or yttrium, has been investigated in the last two decades due to its interesting properties that make possible its application in the microwave frequency range [4–9]. Several investigations involving substitutions have been performed in order to understand its crystal chemistry, but conclusive general remarks are still not possible [10–13].

From the structural viewpoint, there are some controversies about the structure in which this family crystallizes. The first structural investigation of this family was performed by Brixner [14] who found a simple cubic perovskite structure with the exception of RE = La which presented a distorted tetragonal perovskite structure. After this, Filip'ev and Fesenko observed that for RE = La the structure was orthorhombic [15]. Later the unit cell for RE = La was referred to as monoclinic while for RE = Gd the unit cell was referred to as tetragonal by Von Wittmann [16]. Evdokimov and Menshenina also determined that for RE = La–Sm the unit cell is monoclinic, tetragonal for RE = Eu–Tb and double NaCl ordered perovskite type for RE = Dy–Lu and Y [17]. After this, Henmi *et al* determined by Rietveld analyses of the x-ray diffraction that the structure for all compounds in the series is monoclinic belonging to the space group $P2_1/n$ that corresponds to the tilted system $(a^-a^-c^+)$ [18]. More recently,

the Raman spectra for this compound series was assigned as tetragonal for RE = Y, Gd and Tb and orthorhombic for Re = Sm, Gd and La [10]. Finally, using x-ray powder diffraction, Fu [12] showed that this family crystallizes in a distorted monoclinic structure for RE = La–Sm, tetragonal for RE = Eu–Dy and ordered cubic for RE = Ho and Y, belonging to $I2/m$, $I4/m$ and $Fm\bar{3}m$ space groups, respectively. The fact is that despite the crystalline structure for some compounds in this family being different from the NaCl ordered double cubic perovskite, the distortions are very low, complicating the structure determination. Moreover, all structural phase transitions between these phases are subtle without abrupt changes as shown by Fu [12] in the calculated octahedra tilt.

On this basis, we have employed atomistic simulation to model the $Ba_2RE^{3+}NbO_6$ family at room temperature in a NaCl ordered doubled cubic perovskite structure and derived structures where RE is a lanthanide ion or yttrium, in order to calculate their physical properties and investigate the behavior of these properties at the morphotropic phase boundaries. This procedure has been employed with success to model oxides with perovskite structure as reviewed in [19].

2. Computational methodology

In this work we have performed standard lattice-energy minimization to model the $Ba_2RE^{3+}NbO_6$ compounds using the General Utility Lattice Program (GULP) code [20, 21]. This methodology is based on the assumption of pairwise potentials for all interionic interactions. Thus, the minimum-energy structure is calculated at the fixed space groups in order to fit the experimentally determined unit cell parameters and other physical observables. The relaxation of the unit cell dimensions and atomic coordinates at constant pressure was obtained using a Newton–Raphson procedure together with the BFGS method of updating the Hessian matrix [22]. After relaxation of the structure, several bulk properties, such as elastic and dielectric constants, bulk modulus and lattice energy could be calculated.

The potential adopted for ionic compounds commonly has the form

$$\varphi = \sum_{i>j} \left[\frac{e^2}{4\pi\epsilon_0} \frac{Z_i Z_j}{r_{ij}} + A_{ij} \exp\left(-\frac{r_{ij}}{\rho_{ij}}\right) - \frac{C_{ij}}{r_{ij}^6} \right], \quad (1)$$

where the first term describes the long-range electrostatic interaction between the ions of charge $Z_i e$ and $Z_j e$ separated by a distance r_{ij}; the second term gives the Pauli short-range repulsion and the last term is the induced-dipole attraction. In order to sum the Coulomb term, the Ewald summation [23] was employed. Finally, the superposition of the second and the third terms is called the short-range Buckingham potential, whose parameters A_{ij}, ρ_{ij} and C_{ij} are fitted to reproduce experimental data.

The RE^{3+} ion was treated by a rigid ion model [24] due to its low polarizability. In contrast, the remaining ions were modeled by the shell model proposed by Dick and Overhauser [25], in order to consider the polarization of the other ions. In this model, it is assumed that the ith ion is formed

Table 1. Short-range potential parameters for barium, niobium and oxygen ions assumed for $Ba_2RE^{3+}NbO_6$ compounds [26, 27].

	Shell–shell interactions		
	A (eV)	ρ (Å)	C (eV Å^6)
Ba^{2+}–O^{2-}	4818.4160	0.306 700	0.00
Nb^{5+}–O^{2-}	1796.3000	0.345 980	0.00
O^{2-}–O^{2-}	25.4100	0.693 700	32.32
	Core–shell interactions		
	k (eV Å^{-2})	Y ($|e|$)	
Ba^{2+}	34.05	1.831 00	
Nb^{5+}	1358.58	−4.497 00	
O^{2-}	20.53	−2.513 00	

by a massless shell with charge Y_i and a core with mass m_i and charge $X_i = Z_i - Y_i$, where Z_i is the ion valence. To obtain a finite polarizability of the ions, the core is connected to the shell by a harmonic spring whose force constant is k_i.

In our simulations, for the Ba^{2+}–O^{2-}, Nb^{5+}–O^{2-} and O^{2-}–O^{2-} interactions, we have employed interionic potential parameters found in the literature [26, 27]. To describe the RE^{3+}–O^{2-} interaction, we consider potential parameters that could describe better the dielectric constant of these compounds.

3. Results and discussions

3.1. Potential derivation

Initially, in order to obtain the interionic potentials of $Ba_2RE^{3+}NbO_6$ compounds, we firstly have assumed the Ba^{2+}–O^{2-}, Nb^{5+}–O^{2-} and O^{2-}–O^{2-} Buckingham and Ba^{2+}, Nb^{5+} and O^{2-} core–shell potentials listed in the literature [26, 27], which are given in table 1.

The interaction between RE^{3+} and oxygen ions was initially modeled through the potential data presented by Lewis and Catlow [28]. However, these good potential data do not fit well the structural and dielectric data of the investigated materials. Thus, taking the RE = La interaction and optimizing its potential, in order to reproduce the structure and dielectric constant of the Ba_2LaNbO_6 compound, we have obtained the remaining RE^{3+}–O^{2-} interactions, using the recursive relationship given by (2) [29, 30].

$$A_i = A_j \exp\left(\frac{R_i - R_j}{\rho}\right) \quad (2)$$

where R_i is the ionic radius of the lanthanide ion. Finally, the found potentials were refined in order to adjust simultaneously the best possible experimental structural data and dielectric constants. The final potential data obtained for these interactions are given in table 2 together with the tolerance factor t calculated with basis in the RE^{3+} ionic radius [31]. The tolerance factor is a geometrical parameter defined by Goldschmidt [1] for the ABO_3 perovskite compounds as follows

$$t = \frac{R_A + R_O}{\sqrt{2}(R_B + R_O)}. \quad (3)$$

Table 2. Potential parameters for the RE^{3+}–O^{2-} short-range interactions used in this work.

Ion	t	A (eV)	ρ (Å)
La	0.952	806.83	0.371 755
Ce	0.957	865.62	0.363 607
Pr	0.961	941.48	0.355 825
Nd	0.900	970.25	0.352 981
Pm	0.965	1023.72	0.347 135
Sm	0.968	1081.88	0.343 001
Eu	0.970	1156.72	0.337 617
Gd	0.972	1204.60	0.334 137
Tb	0.976	1320.19	0.326 753
Dy	0.978	1374.80	0.323 547
Ho	0.981	1483.38	0.318 034
Y	0.981	1463.80	0.318 857
Er	0.983	1568.57	0.314 192
Tm	0.985	1658.11	0.310 074
Yb	0.988	1782.54	0.304 980
Lu	0.990	1841.37	0.302 250

In the case of double ordered perovskites, this can be rewritten as

$$t = \frac{R_A + R_O}{\sqrt{2}\left(\left(\frac{R_{B'} + R_{B''}}{2}\right) + R_O\right)}. \quad (4)$$

This parameter indicates how far from ideal packing the ionic sizes can move and the structure still remain as a perovskite [2]. Recently, useful correlations have been found between it and device-oriented physical properties of the materials, see for example [8, 9, 32]. Thus, it is interesting to investigate the dependence of this parameter on the physical properties and potential parameters. The behavior permits us to tailor the mixed materials to obtain the desired properties.

It is interesting to note that the structural check was also performed for the pseudocubic parameters calculated by [4]. Moreover, the structural adjust was good even for the compounds with monoclinic and tetragonal structures cited in [12], as we show in table 3. In this table we show the percentage error between experimental and calculated structural parameters. The low errors confirm the good reliability of the potential.

In figure 1 we show the ionic radius dependence on the short-range potential intensity A and range ρ.

As pointed out by Senyshyn *et al* [33], the increase in ρ and the decrease in A demonstrate the so-called 'lanthanide stiffness' effect, where the atomic radius of the rare-earth elements decreases with increase of the atomic number. It is interesting to point out that ρ increases linearly with the RE^{3+} ionic radius and the A parameter has a sigmoidal decay behavior, as the adjusts indicate. This nonlinear behavior is imposed by the Pauli repulsion that inhibits the electronic shell superposition when the lanthanide ionic radius increases such that the sum of oxygen (R_O) and lanthanide (R_{RE}) ionic radii is of the order of the ionic distance in the REO_6 octahedra. Thus, as the sigmoidal (Boltzmann) curve has a lower level constant it adjusts well for this behavior. In order to clarify this, figure 2 shows the A dependence on the sum ($R_O + R_{RE}$). As we can note, the constant lower limit is imposed at distances in the proximity of the higher experimental ($R_O + R_{RE}$) distance obtained, which is 2.461 Å, measured for the Ba_2LaNbO_6 [12].
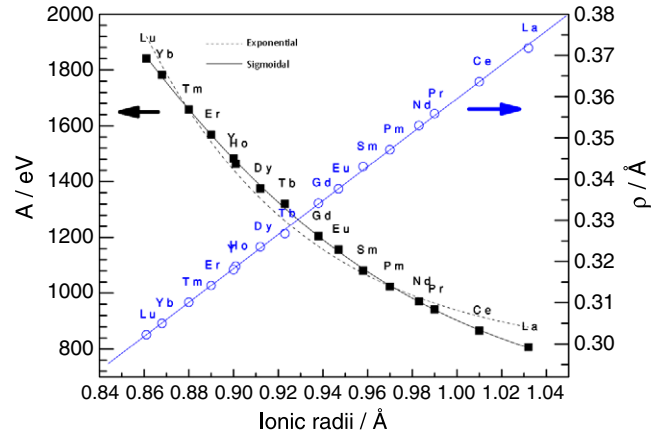
Figure 1. The dependence of short-range potential parameters on the rare-earth ionic radius for the RE^{3+}–O^{2-} interaction.

Table 3. Percentual error between calculated and experimental [4, 12] structural data for the investigated $Ba_2RE^{3+}NbO_6$ compounds.

Ion	t	Pseudocubic axis [4] Δa	Monoclinic [12] Δa	Δb	Δc	$\Delta\theta$
La	0.952	0.04	0.14	0.22	1.08	0.03
Ce	0.957	—	—	—	—	—
Pr	0.961	0.05	—	—	—	—
Nd	0.900	0.05	0.70	0.03	0.13	0.03
Pm	0.965	—	—	—	—	—
Sm	0.968	0.05	—	—	—	—

Ion	t	Δa	Tetragonal [12] Δa	Δc
Eu	0.970	0.05	—	—
Gd	0.972	0.05	0.23	0.20
Tb	0.976	0.02	0.26	0.04
Dy	0.978	0.06	—	—

Ion	t	Δa	Cubic [12] Δa
Ho	0.981	0.06	—
Y	0.981	0.06	0.40
Er	0.983	—	—
Tm	0.985	—	—
Yb	0.988	0.07	—
Lu	0.990	—	—

Good reliability of the assumed potential is given by the comparison between the measured [4] and calculated dielectric constants. This comparison is given in table 4. Once we have good potentials, we can calculate several physical properties of the compounds. In the next section we present the calculated physical properties and emphasize their behavior at the morphotropic phase boundaries (MPB).

3.2. Property calculations

The independent coefficients of the elastic constant tensors for the cubic, monoclinic and tetragonal symmetries in which the
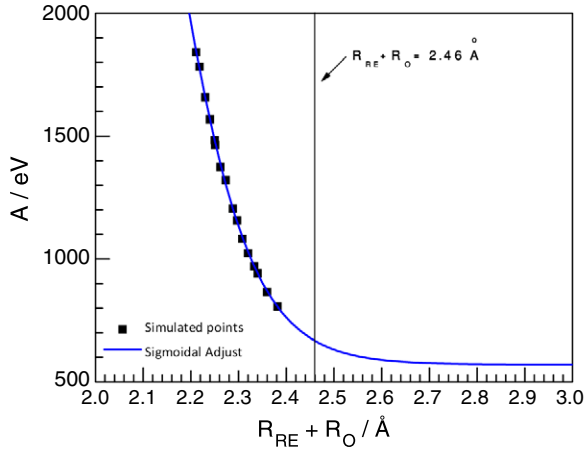
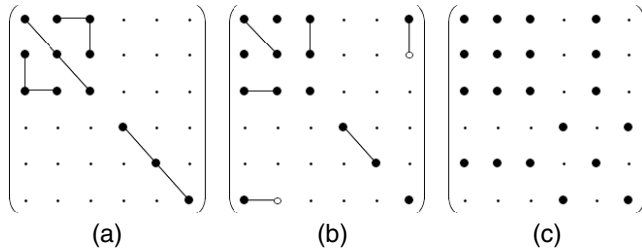**Figure 2.** Short-range potential parameter dependence on the $(R_O + R_{RE})$ sum.

Figure 3. Independent tensor components of the elastic constant tensor for the (a) cubic, (b) tetragonal and (c) monoclinic symmetries in which $Ba_2RE^{3+}NbO_6$ compounds crystallize. The Nye notation [34] has been used, where the symbol • indicates a non-zero component, · indicates a zero component, two • connected by a line indicates two components numerically equal and • connected by a line to a ○ indicates two components whose moduli are equal but opposite in sign.

Table 4. Comparison between the measured [4] and calculated dielectric constants for the investigated $Ba_2RE^{3+}NbO_6$ compounds.

RE^{3+}	t	Calculated	Measured
La	0.952	45.00	45
Ce	0.957	48.77	—
Pr	0.961	44.50	44.5
Nd	0.962	44.00	44
Pm	0.965	49.28	—
Sm	0.968	43.01	43
Eu	0.970	40.00	40
Gd	0.972	40.00	40
Tb	0.976	39.00	39
Dy	0.978	38.90	38.9
Ho	0.981	38.00	38
Y	0.981	36.99	37
Er	0.983	35.36	—
Tm	0.985	35.85	—
Yb	0.988	36.00	36
Lu	0.990	39.27	—

$Ba_2RE^{3+}NbO_6$ compounds crystallize are shown in figure 3. In this figure we used the Nye notation [34].

In figure 4 we show these elastic constant coefficients for all the investigated $Ba_2RE^{3+}NbO_6$ compounds. As we can
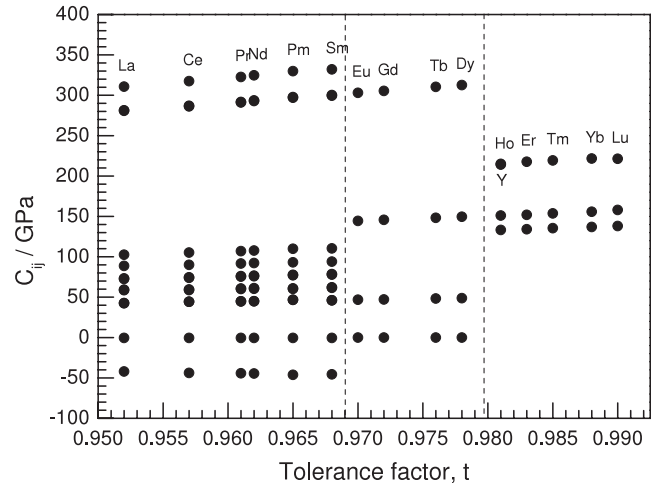

Figure 4. Calculated independent coefficients of the elastic constant tensor for the investigated $Ba_2RE^{3+}NbO_6$ compounds.
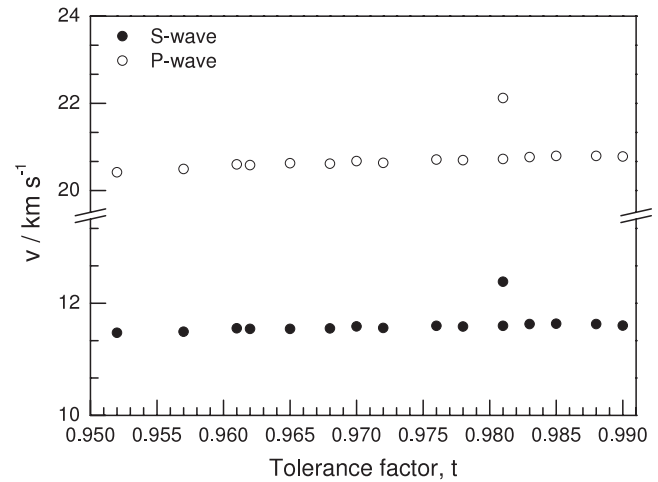

Figure 5. Calculated wave velocities for the investigated $Ba_2RE^{3+}NbO_6$ compounds.

see, they increase subtly with the tolerance factor. This linear behavior is similar to that observed for the elastic constants under low-pressure induced lattice changes and implies a linear behavior of all observables that depends on the elastic constant in the limit of lower lattice distortions. It is interesting to note that both MPBs between cubic and tetragonal phases and tetragonal and monoclinic phases are clear.

These contours are not clear in other properties, such as the S and P wave velocities, given in figure 5. These velocities are practically constant for all compounds. Only for RE = Y are the velocities subtly higher. This effect is due to the low mass of the Y ion in relation to the lanthanide ions.

The bulk modulus shown in figure 6 increases practically linearly with the tolerance factor but does not show the MPBs. The behavior of the bulk modulus is given by

$$B = -525.89 + 711.91t \qquad (5)$$

As the tolerance factor is a purely geometrical parameter, we can tune in the bulk modulus by substituting similar
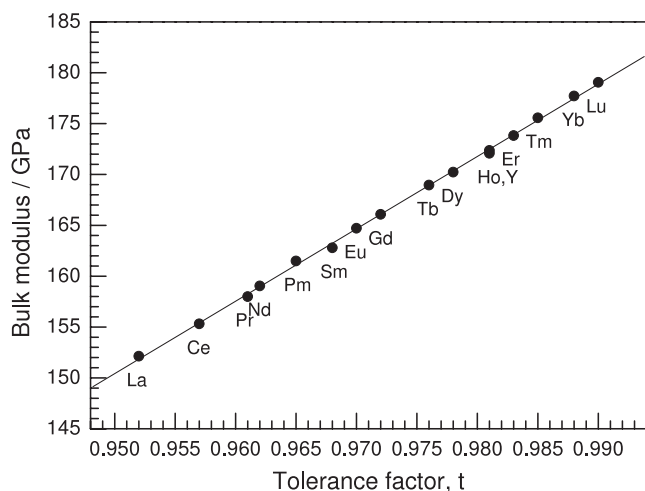
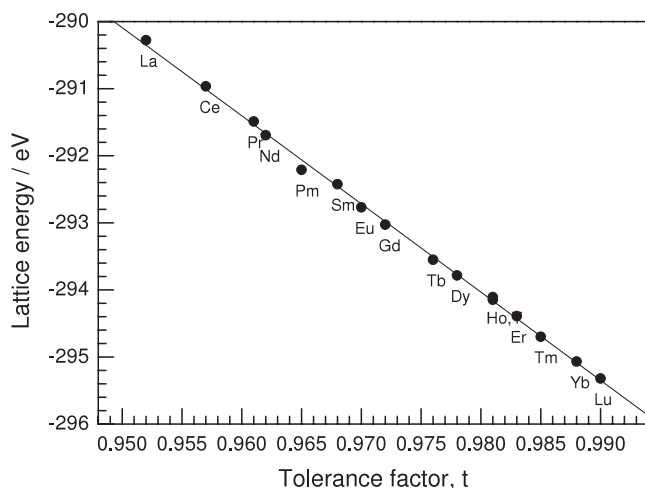**Figure 6.** Calculated bulk modulus for the investigated $Ba_2RE^{3+}NbO_6$ compounds. The line indicates a linear adjust.

Figure 7. Calculated lattice energies for the investigated $Ba_2RE^{3+}NbO_6$ compounds. The line indicates a linear adjust.

ions. This is interesting information for applications as substrates.

The lattice energy also does not show the MPB. This fact reflects the low distortion drives out by the octahedra tilt in relation to the cubic phase. As well as the bulk modulus behavior, the energy dependence on the tolerance factor is also linear. But, in this case, there is a linear decrease in relation to the increase of the tolerance factor, as shown in figure 7.

The relation between tolerance factor and lattice energy is

$$E_L = -165.25 - 131.41t. \tag{6}$$

4. Concluding remarks

In this work we have used a static simulation method to investigate the dependence of the physical properties of the $Ba_2RE^{3+}NbO_6$ (RE^{3+} = La, Ce, Nd, Pr, Pm, Sm, Eu, Gd, Tb, Dy, Y, Ho, Er, Tm, Yb and Lu) compounds on the tolerance factor. The model adopted describes very well the structural

and dielectric properties of the compounds. The parameter that describes the short-range intensity of the interaction between the lanthanide and oxygen ions has a sigmoidal decrease imposed on the approximation of these ions. The parameter that describes the range in this interaction increases linearly. Both behaviors demonstrate the lanthanide stiffness effect. The calculated lattice energy, bulk modulus and sound velocities do not show the morphotropic phase boundaries between cubic, tetragonal and monoclinic phases in which these compounds crystallize. Moreover, the elastic constant coefficients show clearly the MPB.

References

[1] Goldschmidt V M 1927 *Geochemisce Verterlungsgesetze der Elemente* (Oslo: Norske Videnskap)
[2] Bhalla A S, Guo R Y and Roy R 2000 *Mater. Res. Innov.* **4** 3
[3] Kreuer K D 2003 *Annu. Rev. Mater. Res.* **33** 333
[4] Khalam L A, Sreemoolanathan H, Ratheesh R, Mohanan P and Sebastian M T 2004 *Mater. Sci. Eng.* B **107** 264
[5] Kim H S, Kim J H, Choo W K and Setter N 2001 *J. Eur. Ceram. Soc.* **21** 1665
[6] Petzelt J, Zurmuhlen R, Bell A, Kamba S, Kozlov G V, Volkov A A and Setter N 1992 *Ferroelectrics* **133** 205
[7] Zurmuhlen R, Colla E, Dube D C, Petzelt J, Reaney I, Bell A and Setter N 1994 *J. Appl. Phys.* **76** 5864
[8] Zurmuhlen R, Petzelt J, Kamba S, Voitsekhovskii V V, Colla E and Setter N 1995 *J. Appl. Phys.* **77** 5341
[9] Zurmuhlen R, Petzelt J, Kamba S, Kozlov G, Volkov A, Gorshunov B, Dube D, Tagantsev A and Setter N 1995 *J. Appl. Phys.* **77** 5351
[10] Dias A, Khalam L A, Sebastian M T, William C, Paschoal C W A and Moreira R L 2006 *Chem. Mater.* **18** 214
[11] Moreira R L, Khalam L A, Sebastian M T and Dias A 2007 *J. Eur. Ceram. Soc.* **27** 2803
[12] Fu W T and Ijdo D J W 2006 *J. Solid State Chem.* **179** 1022
[13] Gregora I, Petzelt J, Pokorny J, Vorlicek V and Zikmund Z 1995 *Solid State Commun.* **94** 899
[14] Brixner L 1960 *J. Inorg. Nucl. Chem.* **15** 352
[15] Filip'ev V S and Fesenko G E 1961 *Kristallografiya* **6** 770
[16] Wittmann U, Rauser G and Kemmlersack S 1981 *Z. Anorg. Allg. Chem.* **482** 143
[17] Evdokimov A A and Menshenina N F 1982 *Zh. Neorg. Khim.* **27** 2137
[18] Henmi K, Hinatsu Y and Masaki N M 1999 *J. Solid State Chem.* **148** 353
[19] Islam M S 2000 *J. Mater. Chem.* **10** 1027
[20] Gale J D 1997 *J. Chem. Soc. Faraday Trans.* **93** 629
[21] Gale J D and Rohl A L 2003 *Mol. Simul.* **29** 291
[22] Press W H, Teukolsky S A, Vetterling W T and Flannery B P 1992 *Numerical Recipes in Fortran 77* (Cambridge: Cambridge University Press)
[23] Tosi M P 1964 *Solid State Phys.—Adv. Res. Appl.* **16** 1
[24] Valerio M E G, Jackson R A and de Lima J F 2000 *J. Phys.: Condens. Matter* **12** 7727
[25] Dick B G and Overhauser A W 1958 *Phys. Rev.* **112** 90
[26] Pirovano C, Islam M S, Vannier R N, Nowogrocki G and Mairesse G 2001 *Solid State Ion.* **140** 115

[27] Bush T S, Gale J D, Catlow C R A and Battle P D 1994 *J. Mater. Chem.* **4** 831

[28] Lewis G V and Catlow C R A 1985 *J. Phys. C: Solid State Phys.* **18** 1149

[29] Banerjee A, Adams N, Simons J and Shepard R 1985 *J. Phys. Chem.* **89** 52

[30] Woodley S M, Battle P D, Gale J D and Catlow C R A 2003 *Chem. Mater.* **15** 1669

[31] Shannon R D 1976 *Acta Crystallogr.* A **32** 751

[32] Colla I M R E L and Setter N 1994 *Japan. J. Appl. Phys.* **33** 3984

[33] Senyshyn A, Ehrenberg H, Vasylechko L, Gale J D and Bismayer U 2005 *J. Phys.: Condens. Matter* **17** 6217

[34] Nye J F 1985 *Physical Properties of Crystals: Their Representation by Tensors and Matrices* (Oxford: Oxford University Press)